Biosensors and Bioelectronics 32 (2012) 133–140

Contents lists available at SciVerse ScienceDirect

Biosensors and Bioelectronics

journal homepage: www.elsevier.com/locate/bios

Electrochemically amplified molecular beacon biosensor for ultrasensitive DNA sequence-specific detection of *Legionella sp.*

Varun Rai[a], Yin Thu Nyine[a], Hapuarachchige C. Hapuarachchi[b], Hooi Ming Yap[b], Lee Ching Ng[b], Chee-Seng Toh[a,*]

[a] Division of Chemistry and Biological Chemistry, School of Physical and Mathematical Sciences, 21 Nanyang Link, Nanyang Technological University, Singapore 637171, Singapore
[b] Environmental Health Institute, National Environmental Agency, Singapore 138667, Singapore

ARTICLE INFO

Article history:
Received 20 October 2011
Accepted 26 November 2011
Available online 7 December 2011

Keywords:
Molecular beacon
Legionella
Hairpin
DNA biosensor
Electrochemical
Amplification

ABSTRACT

An electrochemically amplified molecular beacon (EAMB) biosensor is constructed using thiolated hairpin DNA-ferrocene probes on gold electrode. The switching from "on" to "off" states of individual probes in the presence of complementary DNA target influences the electrode potential, besides the current, owing to changes in surface density of the electroactive hairpin DNA-ferrocene probes. The EAMB biosensor demonstrates linear range over 8 orders of magnitude with ultrasensitive detection limit of 2.3×10^{-14} M for the quantification of a 21-mer DNA sequence. Its applicability is tested against PCR amplicons derived from genomic DNA of live *Legionella pneumophila*. Excellent specificity down to one and three nucleotides mismatches in another strain of *L. pneumophila* and a different bacterium species, respectively, is demonstrated.

1. Introduction

Methods for the identification of specific nucleic acid sequences have attracted great interest because of the urgent needs to identify and study disease-causing microbes (Lai et al., 2007; Ling et al., 2010; Mishra et al., 2006) contaminated sources including water and food, besides human diseases owing to gene variations (Wang et al., 1998). One method for rapid identification of specific nucleic acid sequences uses direct specific probe-target hybridization (Walker and Rapley, 2000). When coupled to techniques such as piezoelectric (Chen et al., 2010) and surface plasmon resonance (Mrksich et al., 1995), complementary binding of target to surface bound nucleic acids are especially useful because of minimal sample preparation steps. However, these lab-based methods cannot be readily applied at sources of contamination or points-of-care because of bulky equipment and need for stringent laboratory environment. In contrast, electrochemical DNA biosensors have attracted considerable attention because of simple instrumentation, low cost, portability, fast response time, in addition to high specificity and sensitivity which are highly attractive for such on-site analyses (Bini et al., 2007; Tlili et al., 2005; Zhang et al., 2009), with potential for applications in molecular sensing devices (Bergren and McCreery, 2011).

Among the electrochemical detection methods, reported strategies include detection of redox labels physically or covalently attached to the nucleic acid probe or target, such as enzymes (Liu et al., 2008), nano-particles (Wang et al., 2009), metal ions (Wang and Kawde, 2002) and intercalators (Wang et al., 2002) achieved detection of single-base mismatch to some degree. Other approaches include measurement of changes in electrical impedance property of surface film thickness after hybridization (Brett et al., 1999; Oliveira-Brett et al., 2002). Recently, electrochemical hairpin DNA probes show very promising performance in high specificity electrochemical detection down to single-base mismatch using impedance measurement and voltammetric methods (Fan et al., 2003; Gong et al., 2009; Jin et al., 2007; Miranda-Castro et al., 2007). However, the detection limit and sensitivity are considerably poorer than fluorescence molecular beacon probes, which can give high intensity signal arising from rapid turnover of excited and ground states of fluorophore label and a continuous excitation source, thus achieve high signal-to-noise ratio.

In this report, we construct an ultrasensitive electrochemically amplified molecular beacon (EAMB) biosensor by appending reversible ferrocene$^{0/+1}$ redox species at 5′-terminal of hairpin DNA thiolated to gold electrode surface at the 3′-end. Sacrificial redox reagent $Fe(CN)_6^{4-}$ in bulk solution achieves turnover of the oxidation state of surface immobilized hairpin DNA-ferrocene (electrochemical molecular beacon), which amplifies the electrochemical signal output (Scheme 1). This amplification strategy using simple addition of commonly available $Fe(CN)_6^{4-}$ has not

* Corresponding author.
E-mail address: cstoh@ntu.edu.sg (C.-S. Toh).

0956-5663/$ – see front matter © 2011 Elsevier B.V. All rights reserved.
doi:10.1016/j.bios.2011.11.046

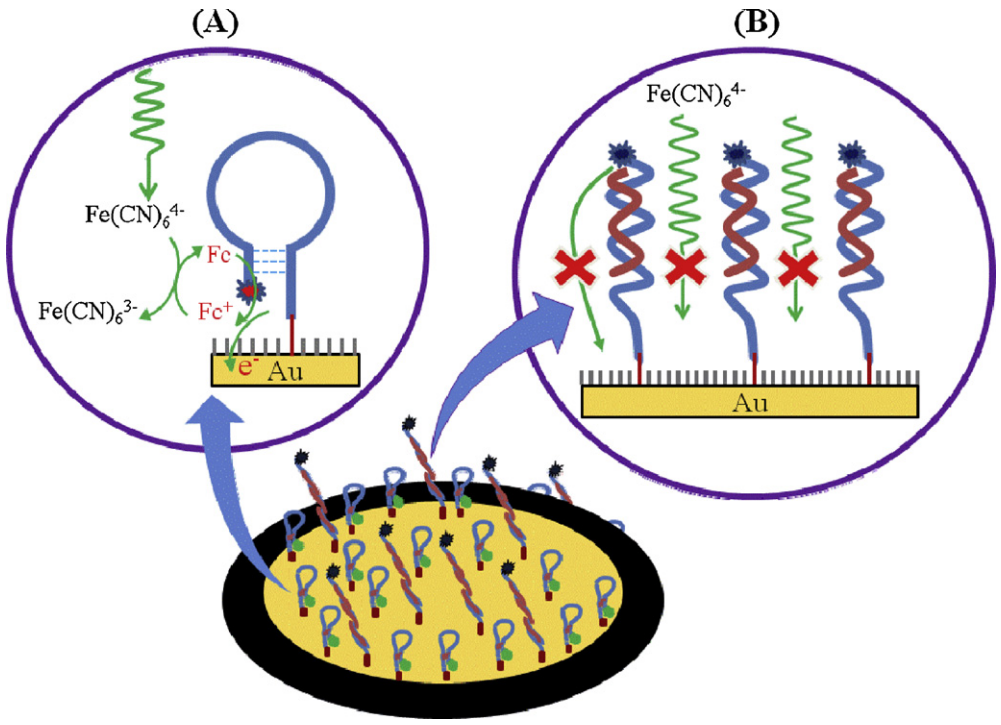

Scheme 1. Scheme of operation for the electrochemically amplified molecular beacon EAMB biosensor. (A) Switched 'ON' amplified biosensor signal response derived from redox cycling of hairpin DNA-ferrocene (Fc) using sacrificial regenerating agent $Fe(CN)_6^{4-}$. (B) Switched 'OFF' biosensor signal response when unfolded DNA duplex forms in the presence of complementary ssDNA target.

been reported in electrochemical hairpin DNA-based biosensors. The EAMB biosensor gives significantly lower detection limit (10^{-14} M) by 1–5 orders of magnitude than non-amplified electrochemical hairpin DNA-based biosensors (Xiao et al., 2006; Xiao et al., 2007; Fan et al., 2003; Long et al., 2004; Gong et al., 2009; Sun et al., 2010) and 6 orders of magnitude lower than electrochemical non-hairpin DNA sensors (Wu et al., 2009).

Herein, the biosensor achieves high specificity differentiation of a 21-mer base sequence from similar sequences with one and three base-pair mismatches. Furthermore, specific detection of label-free genomic sequence of bacterium *Legionella pneumophila* is demonstrated, which presently contaminates ~4% of all potable water sources, causing a serious form of pneumonia known as Legionnaires' disease or legionellosis. Complete elimination of *Legionella* bacteria is extremely difficult owing to widespread intracellular growth in protozoa of biofilms capable of surviving extreme conditions. Thus, the development of a rapid and accurate identification method will be extremely useful in monitoring quality of water sources with high risks of contamination by *Legionella* bacteria, especially during epidemic situations.

2. Material and methods

2.1. Reagents

3′-Thiolated hairpin DNA probe sequence of *L. pneumophila* (3′-HS-$(CH_2)_3$GCAACT TGT TTT CCC CGC CCCTCTCATAGTT$(CH_2)_6NH_2$-5′), non-thiolated complementary target sequence (5′-ACA AAA GGG GCG GGG AGA GTA-3′), single nucleotide mismatch target sequence (5′-ACA AAA GGAGCG GGG AGA GTA-3′) and three nucleotide mismatch target sequence (-5′-GCA AAA GGG GCG GGG AGA GGG-3′) were obtained from Sigma–Aldrich. 6-Mercapto-1-hexanol, 1.0 M tris (2-carboxy-ethyl) phosphine hydrochloride (Tris buffer) of pH 7.0, ethanol (99%) from Sigma–Aldrich, ferrocenecarboxylic acid (>97%), triethylamine (98%) and N, N-dicyclohexylcarbodiimide from Fluka, sodium bicarbonate (Kanto Chemical), dimethylsulfoxide (MP Biomedicals) were used as received. All target analyte solutions were prepared using 1.0 M Tris buffer pH 7.0.

2.2. Design of hairpin DNA-ferrocene probe

A DNA sequence with labile short stem comprising 6-base-pairs and a loop with 16 bases is designed to give a hairpin configuration with theoretical T_m of 27.4 °C and 27.0 °C calculated using nearest Neighbour thermodynamics based software for prediction of nucleic acids folding, under the condition of 1 M Na^+ and folding temperatures of 25 and 30 °C respectively (Zuker, 2003) (see supporting information Fig. S-7 for the predicted stem structure). A GC base sequence is added to the 3′-end to further reduce ease of unfolding of the stem owing to dipole–charge interaction with water molecules (Chattopadhyaya and Isaksson, 2005). The three-carbon organic thiol linker attached to the 3′-end helps anchor the thiolated hairpin to the gold surface via the formation of thermodynamically stable gold–thiol bond. This linker, together with the extra GC base sequence, allows the stem and loop sequences to protrude above the 6-carbon MCH monolayer into the aqueous solution to interact with target DNA. At the 5′-end, ferrocene moiety is attached to a 6-carbon organic linker in order to position the redox moiety close to the gold surface with estimated closest approach distance of ~0–0.35 nm depending on the orientation of ferrocene for facile electron transfer. This presumes the hydrophobic nature of ferrocene and organic linker allows penetration through the MCH monolayer.

A 21-mer target sequence from the *L. pneumophila* genome was searched using National Centre for Biotechnology Information (NCBI) Nucleotide BLAST (Basic Local Alignment Search Tool) resources because of its appropriate length and specificity. The 21-mer DNA target sequence on the *fth*A gene (minus strand) shared by the Corby, Philadelphia1 and Paris strains of *L. pneumophila* was

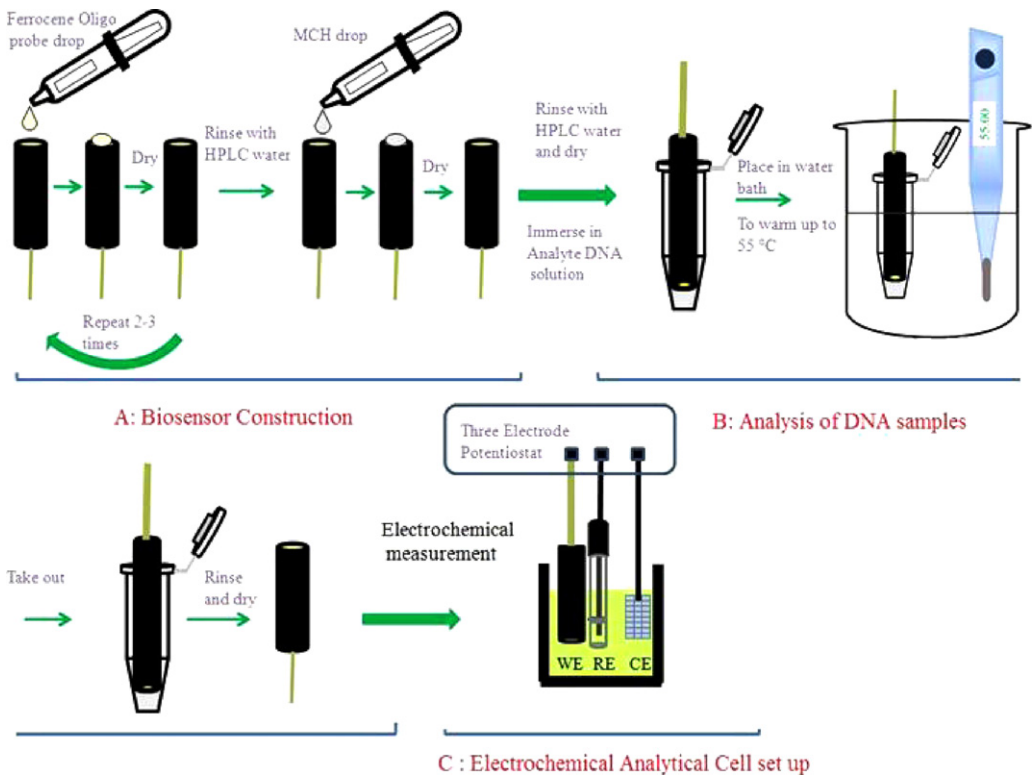

Fig. 1. Schematic of (A) EAMB Biosensor preparation procedure, (B) analytical procedure of analyte DNA sample and (C) electrochemical analytical cell set up.

selected for the 16-base loop sequence with 5-base incorporated into the labile stem of the hairpin probe. Differentiation between these strains and the Lens strain with single-base mismatch and another bacteria species (*Aeromonas hydrophila* subsp. hydrophila ATCC 7966) with three-points mismatch was investigated (Fig. 1).

3. Results and discussion

3.1. The EAMB biosensor

In this work, we first construct surface tethered-hairpin DNA probes tagged with redox active ferrocene, on gold electrode surface. The signal response of the EAMB biosensor is amplified using $Fe(CN)_6^{4-}$ as a sacrificial redox species to regenerate the reduced state of the DNA-ferrocene probe (Scheme 1). In general, such redox cycling scheme relies on rapid homogeneous electron transfer between the regenerating agent and ferrocene, slow heterogeneous reaction of regenerating agent and significantly higher concentration of regenerating species compared to ferrocene (Bergren and Porter, 2005). Using this approach, amplification of Faradaic current response can be achieved with lowered detection limits of ferrocene-based analytes (Bergren and Porter, 2005). Herein, we use surface-attached DNA-ferrocene instead of solution ferrocenes.

Fig. 2A shows the significantly reduced voltammetric peak current of a MCH-hairpin DNA without ferrocene, self-assembled onto gold electrode towards 1 mM $Fe(CN)_6^{4-}$, compared to an uncoated electrode. The hydrophobic MCH adlayer prevents non-specific interactions of DNA target with the electrode, besides acting as a selective interface (Bergren and Porter, 2005) for the redox label ferrocene attached to surface tethered hairpin DNA in the presence of solution $Fe(CN)_6^{4-}$. Interestingly, a large ΔE_p of ~330 mV at the control electrode coated with monolayer of MCH and hairpin DNA without ferrocene is observed, which suggests a strong kinetic limitation in contrast to the Nernstian diffusion-limited behavior at the uncoated electrode. We estimate the heterogeneous rate constant of ferrocyanide at the hairpin-MCH coated electrode using the general equation (Bard and Faulkner, 2000) for an irreversible process is $\sim 1.49 \times 10^{-7}$ cm s^{-1}. This is similar to the dodecane thiolated gold electrode surface (2×10^{-7} cm s^{-1}) (Bergren and Porter, 2005) and at least ~5 orders of magnitude lower than the rate constant of $k = 0.05$ cm s^{-1} estimated using Nicholson method (Nicholson, 1965) for the uncoated gold electrode with reversible voltammetric behavior ($\Delta E_p \sim 64$ mV at 100 mV s^{-1}). When ferrocene labeled hairpin DNA probes are adsorbed onto the electrode surface instead of unlabeled hairpin DNA, a large signal response towards $Fe(CN)_6^{4-}$ similar to the uncoated electrode is achieved (Fig. 2B). Overall, this confirms the mass transfer limited electrodic reaction of ferrocyanide can occur through redox turnover of surface adsorbed ferrocene, while direct reaction of $Fe(CN)_6^{4-}$ at the MCH-coated electrode surface is severely limited.

We evaluate the maximum amplification that can be achieved for the biosensor by comparing theoretical voltammetric peak currents given for a reversible one-electron oxidation of solution $Fe(CN)_6^{4-}$ to surface adsorbed ferrocene, as follows:

$$\frac{i_{p,amplified}}{i_{p,unamplified}} = \frac{2.69 \times 10^5 n^{3/2} A D^{1/2} C \nu^{1/2}}{\alpha F^2 A \nu \Gamma / 2.718 RT} \quad (1)$$

where D is the diffusion coefficient of $Fe(CN)_6^{4-}$, C is the bulk concentration of $Fe(CN)_6^{4-}$, ν is the scan rate and Γ is surface coverage of hairpin DNA-ferrocene and rest of the parameters have their usual meanings.

Under the optimized experimental conditions used in this work, Eq. (1) predicts an amplification factor of ~1300 at average maximum surface coverage of ferrocene of 2×10^{-11} mol cm^{-2} measured from charge passed during linear potential sweep. This is two times higher than the theoretical amplification factor of a homogeneous mixture of ferrocene and $Fe(CN)_6^{4-}$ (Bergren and Porter, 2005). The experimental amplification factor extracted from Fig. 2B is however significantly lower at ~130. The origin of this disparity between theoretical and experimental amplification

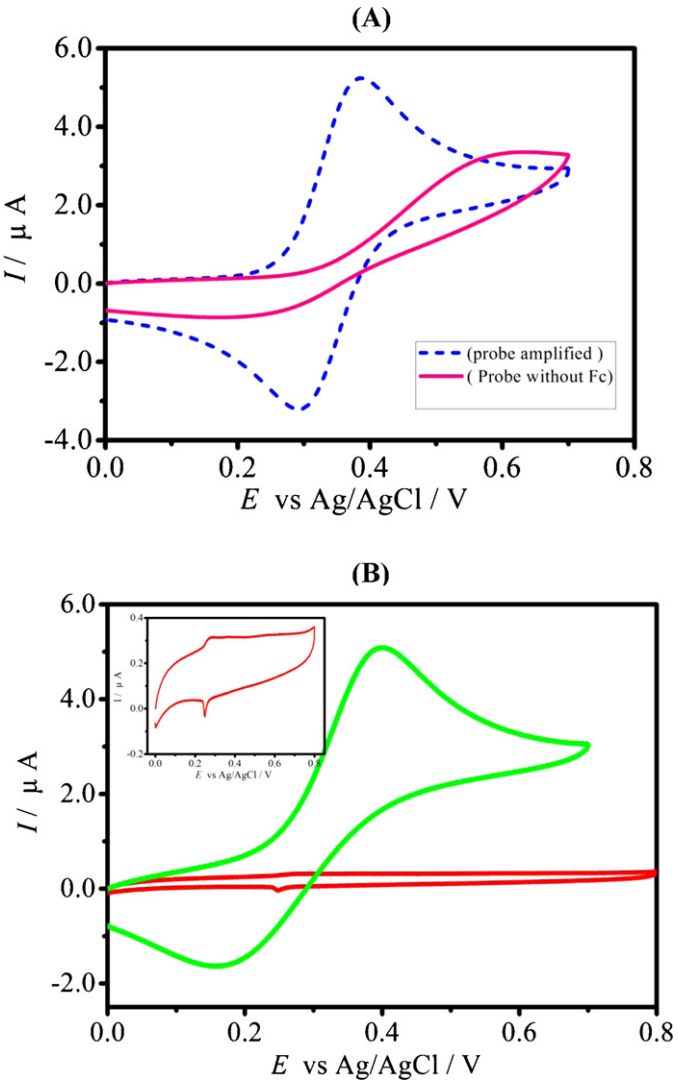

Fig. 2. (A) Cyclic voltammogram of bare gold electrode ( ) and gold electrode immobilized with hairpin DNA without ferrocene (Fc) and MCH ( ) in presence of 1 mM $Fe(CN)_6^{4-}$. (B) Cyclic voltammogram of gold electrode immobilized with hairpin DNA probes in the absence ( ) and presence ( ) of 1 mM $Fe(CN)_6^{4-}$. Inset: magnified view of Faradaic current peaks of hairpin DNA-ferrocene probes in the absence of $Fe(CN)_6^{4-}$.

factors could arise from poor mediation efficiency (Bergren and Porter, 2005) or insufficient amount of $Fe(CN)_6^{4-}$ to support the fast mediation and rapid turnover of surface ferrocene. To verify this, we increase the $Fe(CN)_6^{4-}$ concentration by 10 and 100 times (see supporting information Fig. S-2 which shows corresponding 9 and 50 times rise in peak currents, respectively). This indicates redox recycling of surface ferrocene is limited by $Fe(CN)_6^{4-}$ concentration from 1 to 100 mM $Fe(CN)_6^{4-}$. Though larger signals can be derived in higher $Fe(CN)_6^{4-}$ concentrations, the higher background currents due to $Fe(CN)_6^{4-}$ do not significantly improve the linear range nor detection limit of the biosensor. On the other hand, a closer agreement of theoretical and experimental amplification factor can also be achieved by lowering surface coverage of ferrocene (Bergren and Porter, 2005). However, this gives poorly defined voltammogram in absence of $Fe(CN)_6^{4-}$, and most critically, intermediate surface coverage cannot be easily reproduced. Thus, DNA-ferrocene probes are self-assembled on gold electrode surface over ~3–4 days to achieve maximum surface coverage. This method is used during all biosensor preparation and 1 mM $Fe(CN)_6^{4-}$ is used in all biosensing solution.

3.2. Biosensor signals derived from differential pulse voltammetry

Because large capacitive currents are encountered during potential cycling of the highly charged hairpin ferrocene probes, extraction of reproducible peak currents under identical experimental conditions is a challenge for ultrasensitive performance of the biosensor. In contrast, differential pulse voltammetry can remove capacitive currents and known to increase detection limits compared to non-pulsed voltammetry by ca. two folds. Supporting information Fig. S-3 shows the significantly sharper peaks derived during DPV scans compared to cyclic voltammetry (Fig. 2).

Fig. 3A shows the corresponding decrease in the biosensor DPV peak current as the concentration of label-free complementary target increases. An interesting and analytically useful attribute of this biosensor is that its peak potential also shifts with increasing target concentration. Shift in voltammetric potential can arise from variation in the heterogeneous rate constant of a redox species, owing to changes in the surface density of redox active sites (Koh et al., 2007). If each surface tethered hairpin DNA probe tagged with a redox species such as ferrocene is treated as a nanosized electroactive site, then binding with its complementary target help quench its electrochemical activity and reduces the overall surface coverage of redox active hairpin DNA-ferrocene sites on the electrode. Thus, we use Langmuir isotherm to describe the binding of target DNA to the hairpin DNA-ferrocene probe. Because the target-probe binding changes probe surface coverage and reduces the heterogeneous rate constant of ferrocene, it is possible to derive an analytically useful relation involving the DPV peak potential of the EAMB biosensor, the probe-target equilibrium binding constant K and complementary DNA target concentration C (see Note S-4):

$$E_p - E_{p,o} = A\ \ln(1 + KC) \tag{2}$$

where $E_{p,o}$ and E_p refer to the DPV peak potentials of the EAMB biosensor before and after hybridization with target DNA, respectively and A is an arbitrary constant.

Besides potential, the surface coverage of electroactive hairpin DNA-ferrocene θ also influences the biosensor current signal. Using similar Langmuir isotherm approach as a nanoporous biosensor we described previously (Nguyen et al., 2009), the biosensor current signal normalized against the maximum current signal obtained in the absence of target, can be related to target concentration as follows:

$$\frac{I_{DNA}}{I_0} = \frac{1 - (I_{background}/I_0)}{1 + KC} + \frac{I_{background}}{I_0} \quad \text{or}$$

$$\frac{I_{DNA}}{I_0} = \frac{1 + (I_{background}/I_0)KC}{1 + KC} \tag{3}$$

where I_{DNA} and I_0 are biosensor current signals in the presence and absence of target DNA; $I_{background}$ is the minimum biosensor current signal due to background $Fe(CN)_6^{4-}$ obtained at high concentrations of target DNA; K is the binding equilibrium constant between hairpin probe and target DNA and C is the complementary target concentration.

Practically, the current signal or peak potential yields linear responses with respect to the logarithm of the complementary ssDNA target concentration when normalized or offset against the blank solution without any complementary target, respectively. Non-linear curve fits of Eqs. (2) and (3) to experimental data of the normalized biosensor current signal and offset peak potential responses, give relatively good agreements (Fig. 3B and C). Interestingly, replacing KC with $(KC)^{1/n}$ in Eqs. (2) and (3) improves the non-linear curve fit further. Nucleic acid bases and polynucleotides are known to exhibit stacking association in aqueous solutions due to hydrophobic interactions (Voet and Voet, 1990). Subsequent dissociation of stacked ssDNAs into n single strands

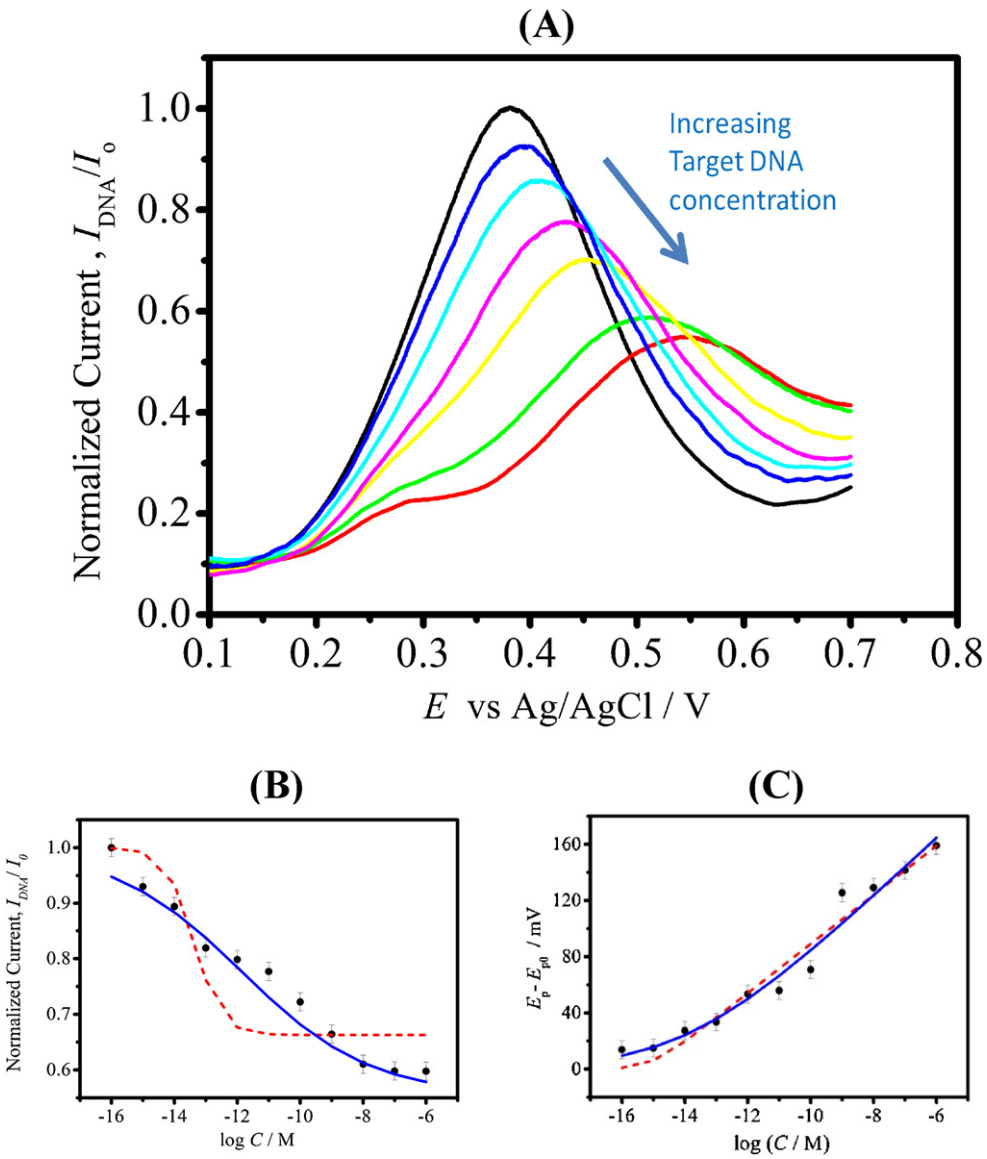

Fig. 3. (A) Biosensor current response towards increasing concentration of complementary target: 10^{-16}, 10^{-14}, 10^{-12}, 10^{-10}, 10^{-08} and 10^{-06} M. Plots showing (B) averaged normalized current signal best fitted to Eq. (3) and (C) averaged peak potential response best fitted to Eq. (2), derived from three biosensors. (●) Experiment data, (▬ ▬ ▬) nonlinear best fit, (▬▬) nonlinear best fit using $(KC)^{1/n}$ instead of KC in Eqs. (2) and (3). Error bars and points represent average standard deviations derived from three biosensors. Sharp decrease in current response from 10^{-16} to 10^{-14} M is due to loss of molecular beacon probes during the first two measurements at 10^{-16} and 10^{-15} M (see Notes S-2).

before binding to the hairpins, requires that the binding rate is proportional to the n power of the number of hairpin sites thus give rise to $(KC)^{1/n}$. Consequently, the binding affinity K values derived from best fitted current signal and peak potential responses were $7.5 \pm 7.0 \times 10^{11}$ M^{-1} ($n = 4.8 \pm 0.7$) and $7.6 \pm 20.7 \times 10^{13}$ M^{-1} ($n = 4.0 \pm 1.6$) respectively. This close agreement within one order of magnitude between the experimental and theoretical K values of 2.5×10^{12} predicted from free binding energy (SantaLucia, 1998) verifies the simple relations between biosensor responses and surface coverage of hairpin DNA-ferrocene sites. It also strongly suggests a slightly complex situation involving stacked DNA target comprising of four to five oligonucleotides in the measuring solution.

3.3. Biosensing mechanism

The following mechanism explains the current response of the EAMB biosensor (Fan et al., 2003). The DNA-ferrocene undergoes redox reaction at the electrode in the hairpin configuration. In the presence of DNA target under hybridization condition, hairpin DNA-ferrocene probes unfold, bind with target to form the redox inactive duplex DNA structures due to significant change in distance from ~0.3 nm to larger than ~12.3 nm between ferrocene and electrode. The current decreases as concentration of target DNA increases as the duplex structures increase proportionally with respect to the hairpin probes (Fan et al., 2003). At high target concentration, decrease in current is limited by the background current of $Fe(CN)_6^{4-}$, attributed to tunneling current or surface defects in the MCH layer. It is equally possible that significant part of the observed current signal is due to direct reaction of $Fe(CN)_6^{4-}$ at the MCH/DNA probe-covered electrode. In this situation, steric hindrance or electrostatic repulsion of charged $Fe(CN)_6^{4-}$ by the higher negatively charged duplex DNA structures in the adlayer compared to hairpin DNAs can cause decrease in current signal (Gong et al., 2009). However, this mechanism cannot explain the observed potential shift. A control experiment carried out using hairpin DNA

without ferrocene tag (supporting information Fig. S-5A) confirms addition of complementary target does not cause potential shift in the biosensor response though current was observed to decrease in same way as the biosensor containing hairpin DNA-ferrocene which is attributed to charge repulsion effect (Gong et al., 2009). Fig. S-5B shows DPV current response of a second control electrode immobilized with hairpin DNA without ferrocene tag, in the presence of increasing concentration of non-complementary 21 mer polycytosine DNA target. There is no significant change in DPV signal for wide concentration range of 10^{-6} to 10^{-16} M, unlike the biosensor response towards complementary targets (Fig. 3A).

3.4. Analytical performance

Fig. 3B and C shows the plots of biosensor current signal and peak potential responses versus the logarithm of complementary ssDNA target concentration derived from three biosensors with signal amplification in 1 mM $Fe(CN)_6^{4-}$. Excellent linearity with 8 orders of magnitude from 10^{-14} to 10^{-6} M ($R^2 = 0.99$) for current signal and 7 orders of magnitude from 10^{-13} to 10^{-6} M ($R^2 = 0.98$) for peak potential response were obtained, respectively. Detection limit was determined from the minimum DNA concentration which caused the change in current signal or peak potential response equivalent to three times the average background noise in the absence of DNA target. Detection limits for a 21-mer DNA sequence of *L. pneumophila* were 2.3×10^{-14} M (current signal) and 5.9×10^{-13} M (peak potential) respectively, present significant improvement of 5–6 orders over hairpin DNA sensors based on colorimetry (Bockisch et al., 2005), optical (Wei et al., 2005) and fluorescence (Du et al., 2003).

These figures of merit including a relatively rapid analysis time of 45 min presents a significant improvement in DNA detection limits over existing non-pcr methods and is comparable to state-of-the-art enzyme based amplified E-DNA sensor (Liu et al., 2008) and impedimetric DNA sensor (Long et al., 2004). In addition, the used biosensor can be regenerated up to six times with very good reproducible normalized signal response by incubating in a pH 7.0, 0.5 M Tris buffer for 30 min at 75 °C. Average standard error of 2.6% is obtained for one biosensor and for three biosensors, the errors range from 2 to 9%. Further, the additional readout derived from peak potential besides current signal can be useful to distinguish common current signal measurement errors associated with oxidation or reduction of trace impurities which has minimal influence on the peak potential values.

3.5. Specific response towards one and three base-pair mismatches

Fig. 4 shows the normalized current signal and peak potential responses of one EAMB biosensor towards a target containing DNA sequence commonly found in several *L. pneumophila* strains, and two other targets containing similar sequences but with single-base and triple-bases mismatches found in Lens strain *L. pneumophila* and *A. hydrophila*, respectively. During analysis the target was thermostated with biosensor at 55 °C, between the theoretical solution T_m of the complementary sequence and sequence with one-point mismatch which are 60 °C and 42 °C respectively, calculated using nearest Neighbour thermodynamics based software (biomath Tm Calculators). For the sequence with one mismatch in the middle position, T_m is significantly lower than the complementary sequence. This has been explained by the formation of kink at the mismatched position which disrupts complementary binding of the remaining bases in the same sequence (Long et al., 2004). From Fig. 4, it is clear that the complementary target and sequence with one nucleotide mismatch can be easily differentiated, which demonstrates this electrochemically

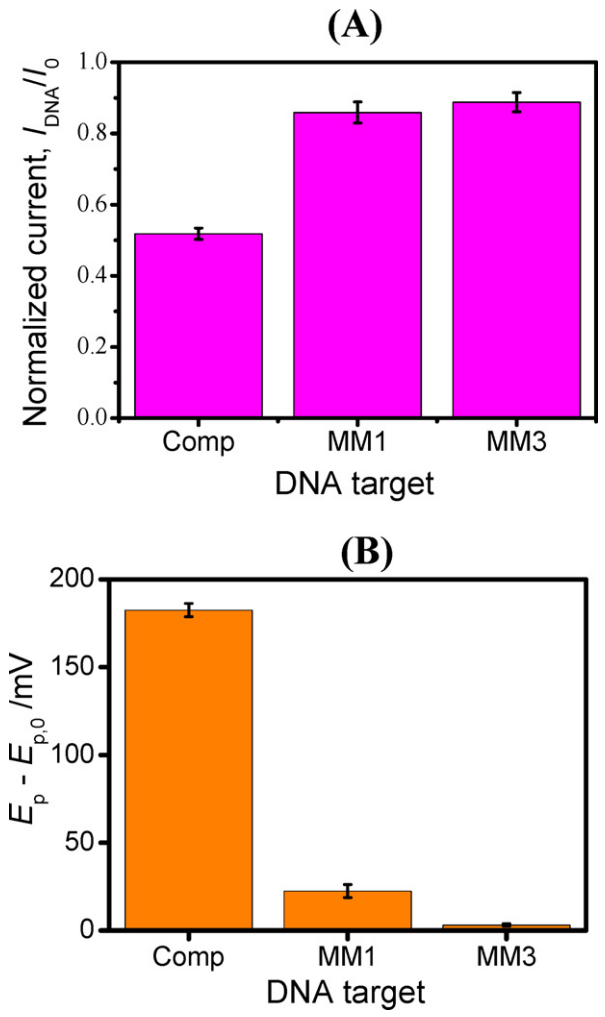

Fig. 4. Changes in (A) normalized current signal and (B) peak potential of the same biosensor towards 1 μM 21-mer complementary target (Comp) and target sequences containing single-base mismatch (MM1) and triple-bases mismatch (MM3) with zero, one and two regeneration procedure (see text), respectively. Error bars correspond to standard deviations obtained from 3 consecutive DPV measurements.

amplified signal of the hairpin DNA probe is highly selective down to single nucleotide mismatch.

To test the limit of this method for further high specificity detection, we introduce 3 nucleotide mismatches at terminal positions 1, 2 and 21. Mismatch of base-pairs at terminal positions form dangling ends instead of kinks (Long et al., 2004), so such 3-points mismatch sequence has a much closer Tm (57 °C) to the complementary sequence thus would be more difficult to distinguish. Very interestingly, at higher hybridization temperature of 55 °C, the 3 base-pair mismatch sequence shows negligible change in biosensor signal response and can be clearly differentiated from the complementary target (Fig. 4). Previous study on terminal mismatch at proximal end of surface tethered DNA sequences indicate enhanced flexibility of the DNA-linker region, likely due to fraying of the strands at the terminal mismatch position (Long et al., 2004) such orientation changes may affect the kinetics of hybridization (Jeffrey et al., 1981) and further influence the selectivity against the mismatch sequence. Consequently, sequences with one and three mismatches have lower T_m than the hybridization temperature 55 °C and do not hybridize well with the probe sequence, giving significant differences in the normalized DPV peak currents and absolute peak potential values (Fig. 4).

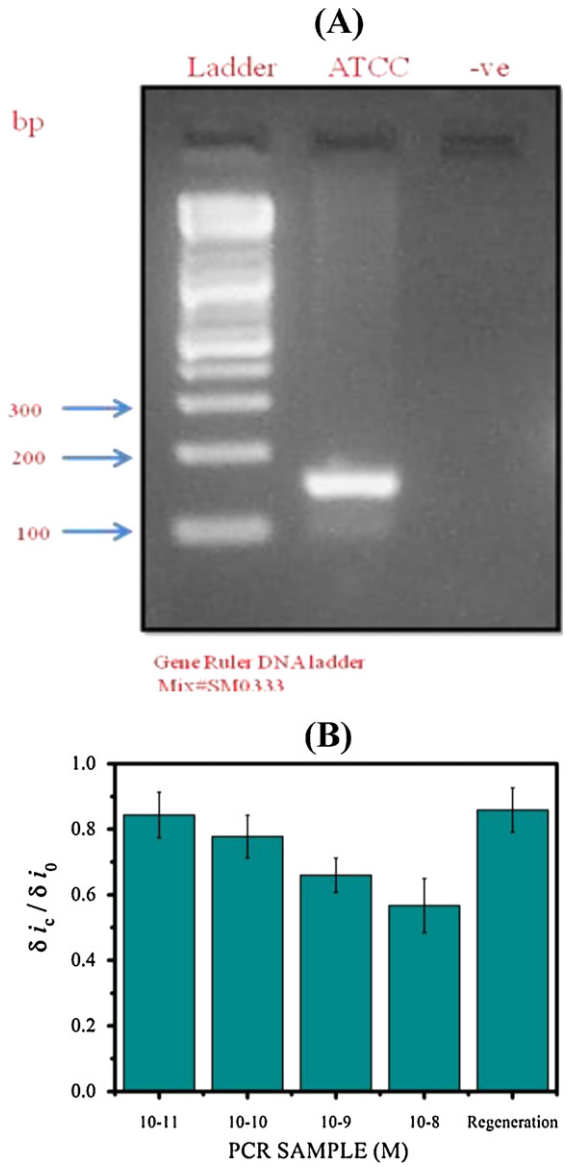

Fig. 5. (A) Electrophoretic analysis of the asymmetric PCR amplification for a 157-bp gene (*flhA*) of *Legionella pneumophila*. (B) Biosensor signal response towards this real time PCR gene sample of *Legionella pneumophila* at 10^{-11}, 10^{-10}, 10^{-9}, 10^{-8} M. Error bars correspond to standard deviations obtained from 3 consecutive DPV measurements.

3.6. Detection of Legionella pneumophila genomic DNA

In order to test the applicability of the EAMB biosensor in real sample analysis, it was challenged with PCR amplicons for *Legionella* genomic DNA. A 157-bp region between position 58 and 78 in the genomic DNA (see Table S-6) was selected as the target, with complementary loop sequence in the hairpin DNA-ferrocene probe of the biosensor. *L. pneumophila* was cultured overnight, and its genomic DNA was isolated using a bacteria genomic DNA isolation kit (Cat#51306 QIAamp DNA Mini Kit). PCR amplification was performed in a PCR cycler (Applied Bio systems Gene Amp PCR system 2700). A pair of asymmetric primers (10 Primer1/1 Primer2) was employed in order to generate the ss-DNA target. The amplification protocol comprises an initial 5 min heating at 95 °C followed by 35 cycles of 95 °C for 30 s, 55 °C for 30 s, and 72 °C for 30 s. The reaction system was further incubated for 5 min at 72 °C to extend any incomplete products. The PCR products were subsequently diluted by 10-fold successively up to four serial dilutions for detection by the biosensor. Fig. 5A shows the gel electrophoretic isolation of the 157 base pair target sequence from the cultured *L. pneumophila* cells and the biosensor signal response towards serial diluted PCR amplicon samples of the isolated target sequence. The biosensor can be regenerated after exposure to the series of diluted PCR amplicon samples using 75 °C, 30 min heating cycle (Fig. 5B).

4. Conclusions

We report a new electrochemically amplified molecular beacon biosensor, made from surface attached thiolated DNA hairpin probes appended to redox active ferrocene species, with electrochemical regeneration by sacrificial $Fe(CN)_6^{4-}$ reagent. Ultrasensitive detection of a label-free 21-mer complementary DNA sequence of *L. pneumophila* at (~20) fM level can be achieved. The EAMB biosensor selectively differentiates between *L. pneumophila* and two other species and shows exceptionally wide linear range derived from DPV current signal from 10^{-14} to 10^{-6} M. The equally responsive biosensor peak potential provides additionally useful quantitative and selective analytical data about the complementary DNA analyte within the linear range from 10^{-13} to 10^{-6} M. The sensitivity of this EAMB biosensor outperforms existing DNA biosensors which do not rely on target amplification methods, shows potential broad applications in DNA-based biosensors for rapid identification and quantification of pathogenic microbes.

Acknowledgements

We thankfully acknowledge financial support from NTU grant and Ministry of Education scholarship for VR.

Appendix A. Supplementary data

Supplementary data associated with this article can be found, in the online version, at doi:10.1016/j.bios.2011.11.046.

References

Bini, A., Minunni, M., Tombelli, S., Centi, S., Mascini, M., 2007. Anal. Chem. 79, 3016–3019.
Bard, A.J., Faulkner, L.R., 2000. Electrochemical Methods: Fundamentals and Application, 2nd ed. John Wiley & Sons, New York, p. 594, pp. 196, 236.
Bergren, A.J., McCreery, R.L., 2011. Annu. Rev. Anal. Chem. 4, 173–195.
Bergren, A.J., Porter, M.D., 2005. J. Electroanal. Chem. 585, 172–180.
Bockisch, B., Grunwald, T., Spillner, E., Bredehorst, R., 2005. Nucleic Acids Res. 33, e101.
Brett, C.M.A., Oliveira Brett, A.M., Serrano, S.H.P., 1999. Electrochim. Acta 44, 4233–4239.
Chattopadhyaya, J., Isaksson, J., 2005. Biochemistry 44, 5390–5401.
Chen, Q., Bian, Z., Hua, X., Yao, C., Wu, W., Zhang, X., Zhang, B., Huang, J., Tang, W., Fu, W., 2010. Biosens. Bioelectron. 25, 2161–2166.
Du, H., Disney, M.D., Miller, B.L., Krauss, T.D., 2003. J. Am. Chem. Soc 125, 4012–4013.
Fan, C., Plaxco, K.W., Heeger, A.J., 2003. Proc. Natl. Acad. Sci. U.S.A. 100, 9134–9137.
Gong, H., Zhong, T., Gao, L., Li, X., Bi, L., Kraatz, H.B., 2009. Anal. Chem. 81, 8639–8643.
Jeffrey, W., Nelson, F.H.M., Ignacio Jr., T., 1981. Biopolymers 20, 2509–2531.
Jin, Y., Yao, X., Liu, Q., Li, J., 2007. Biosens. Bioelectron. 22, 1126–1130.
Koh, G., Agarwal, S., Cheow, P.S., Toh, C.S., 2007. Electrochim. Acta 52, 2815–2821.
Lai, Y.-L., Chung, Y.-K., Tan, H.-C., Yap, H.-F., Yap, G., Ooi, E.-E., Ng, L.-C., 2007. J. Clin. Microbiol. 45, 935–941.
Ling, L.M., Chow, A.L., Lye, D.C., Tan, A.S., Krishnan, P., Cui, L., Win, N.N., Chan, M., Lim, P.L., Lee, C.C., Leo, Y.S., 2010. Clin. Infect. Dis. 50, 963–969.
Liu, G., Wan, Y., Gau, V., Zhang, J., Wang, L., Song, S., Fan, C., 2008. J. Am. Chem. Soc. 130, 6820–6825.
Long, Y.T., Li, C.Z., Sutherland, T.C., Kraatz, H.B., Lee, J.S., 2004. Anal. Chem. 76, 4059–4065.
Miranda-Castro, R., De-Los-Santos-Álvarez, P., Lobo-Castanon, M.J., Miranda-Ordieres, A.J., Tunon-Blanco, P., 2007. Anal. Chem. 79, 4050–4055.
Mishra, S., Raj, D.K., Hazra, R.K., Dash, A.P., Supakar, P.C., 2006. Trans. R. Soc. Trop. Med. Hyg. 100, 243–247.
Mrksich, M., Sigal, G.B., Whitesides, G.M., 1995. Langmuir 11, 4383–4385.
Nguyen, B.T.T., Koh, G., Lim, H.S., Chua, A.J.S., Ng, M.M.L., Toh, C.-S., 2009. Anal. Chem. 81, 7226–7234.
Nicholson, R.S., 1965. Anal. Chem. 37, 1351–1355.
Oliveira-Brett, A.M., Brett, C.M.A., Silva, L.A., 2002. Bioelectrochemistry 56, 33–35.

SantaLucia, J.J., 1998. Proc. Natl. Acad. Sci. U.S.A. 95, 1460–1465.
Sun, C., Zhang, L., Jiang, J., Shen, G., Yu, R., 2010. Biosens. Bioelectron. 25, 2483–2489.
Tlili, C., Korri-Youssoufi, H., Ponsonnet, L., Martelet, C., Jaffrezic-Renault, N.J., 2005. Talanta 68, 131–137.
Voet, D., Voet, J.G., 1990. Biochemistry. Wiley, New York, pp. 1120–1121.
Walker, J.M., Rapley, R., 2000. The Royal Society of Chemistry, 4th ed. Cambridge, U.K, pp. 34–37.
Wang, D.G., Fan, J.-B., Siao, C.-J., Berno, A., Young, P., Sapolsky, R., Ghandour, G., Perkins, N., Winchester, E., Spencer, J., Kruglyak, L., Stein, L., Hsie, L., Topaloglou, T., Hubbell, E., Robinson, E., Mittmann, M., Morris, M.S., Shen, N., Kilburn, D., Rioux, J., Nusbaum, C., Rozen, S., Hudson, T.J., Lipshutz, R., Chee, M., Lander, E.S., 1998. Science 280, 1077–1082.
Wang, G., Zhang, J., Murray, R.W., 2002. Anal. Chem. 74, 4320–4327.
Wang, J., Kawde, A.N., 2002. Analyst 127, 383–386.
Wang, J., Meng, W., Zheng, X., Liu, S., Li, G., 2009. Biosens. Bioelectron. 24, 1598–1602.
Wei, F., Chen, C., Zhai, L., Zhang, N., Xin, S.Z., 2005. J. Am. Chem. Soc 127, 5306–5307.
Wu, J., Huang, C., Cheng, G., Zhang, F., He, P., Fang, Y., 2009. Electrochem. Commun 11, 177–180.
Xiao, Y., Qu, X., Plaxco, K.W., Heeger, A.J., 2007. J. Am. Chem. Soc. 129, 11896–11897.
Xiao, Y., Lubin, A.A., Baker, B.R., Plaxco, K.W., Heeger, A.J., 2006. Proc. Natl. Acad. Sci. U.S.A. 103, 16677–16680.
Zhang, J., Dong, S., Lu, J., Turner, A.P.F., Fan, Q., Jia, S., Lu, X., Yang, H., Qiao, C., Zhou, H., He, G., 2009. Anal. Lett. 42, 2905–2913.
Zuker, M., 2003. Nucleic Acids Res. 31, 3406–3415.